Available online at www.sciencedirect.com
SCIENCE DIRECT®
International Journal of Heat and Mass Transfer 48 (2005) 3736–3752
International Journal of HEAT and MASS TRANSFER
www.elsevier.com/locate/ijhmt

Enhanced saturation and subcooled boiling of FC-72 dielectric liquid

Jack L. Parker, Mohamed S. El-Genk *

Institute for Space and Nuclear Power Studies/Chemical and Nuclear Engineering Department, The University of New Mexico, Albuquerque, NM 87131, United States

Received 15 September 2004; received in revised form 4 March 2005

Abstract

Experiments are conducted which investigated enhancements in nucleate boiling of FC-72 dielectric liquid on porous graphite and compared results with those on a smooth copper surface of the same dimensions (10 × 10 mm). Also investigated is surface temperature excursion at boiling incipience and the obtained values of CHF are compared with those of other investigators on copper, silicon, and micro-finned silicon surfaces and micro-porous coatings. Results showed no temperature excursion at boiling incipience on porous graphite but as much as 14.0 K in saturation and 9.0–13.3 K in subcooled boiling on copper. The nucleate boiling heat transfer coefficients on porous graphite are significantly higher than on copper and the values of CHF (27.3, 39.6, 49.0, and 57.1 W/cm^2 in saturation and at ΔT_{sub} = 10, 20, and 30 K, respectively) are 63–94% higher than on copper (16.9, 21.9, 26.9, and 29.5 W/cm^2, respectively). The surface superheats at CHF on porous graphite (11.0 K in saturation and 17.2–19.5 K in subcooled boiling) are lower than on copper (21.3 K and 22.9–24.9 K, respectively). The nucleate boiling heat transfer coefficient increase with subcooling and CHF increased linearly with ΔT_{sub}. The subcooling coefficient of CHF on porous graphite (0.041) is slightly smaller than those on micro-porous coatings (0.044 and 0.049) but much higher than those on micro-finned silicon surfaces (0.022, 0.036), and on Cu, Si, and enhanced SiO_2 (0.018) surfaces.

Keywords: Porous graphite; CPU chips cooling; Boiling enhancement; Dielectric liquids

1. Introduction

The continuing increases in clock speed of CPU chips and microprocessors increase the dissipated thermal power and develop hot spots on the surface of the chips. The hot spot dissipation heat flux could be two to three times the surface average heat flux, currently ranges from 40 to 60 W/cm^2. According to the 2002 International Roadmap for Semiconductors, the dissipated power by a high performance CPU chip is projected to exceed 160 W in the near future and 250 W by 2010–2013 [1]. Also, the local dissipation heat flux from the IBM power-4 chip is currently near 100 W/cm^2 [1,2]. The high dissipation heat fluxes and non-uniform surface temperature induce mechanical stresses that could damage the chip or shorten its service lifetime. Therefore, it is important to remove the dissipated power

* Corresponding author. Tel.: +1 505 277 5442/2813; fax: +1 505 277 2814.
E-mail address: mgenk@unm.edu (M.S. El-Genk).

0017-9310/$ - see front matter © 2005 Elsevier Ltd. All rights reserved.
doi:10.1016/j.ijheatmasstransfer.2005.03.011

Nomenclature

C	coefficient (Eqs. (2) and (3))
CHF	critical heat flux (W/cm^2)
NHTC	nucleate boiling heat transfer coefficient
g	acceleration of gravity (m/s^2)
h_{fg}	latent heat of vaporization (W/kg)
q	surface heat flux (W/cm^2)
T	temperature (K)

Subscripts

b	liquid pool
ex	excursion
Cu	Copper
CHF	at critical heat flux
NC	natural convection
i	boiling incipience
l	liquid
NB	nucleate boiling
PG	porous graphite
sat	saturation
Si	silicon
sub	subcooling
w	boiling surface
v	vapor

Greek symbols

ΔT_{sat}	surface superheat, $(T_w - T_{sat})$ (K)
ΔT_{sub}	liquid subcooling, $(T_{sat} - T_b)$ (K)
ρ	density (kg/m^3)
σ	surface tension (N/m)

while minimizing the temperature gradient across the surface of the chip. Because of the ever-increasing dissipation power by CPU chips future cooling is likely to transition from being air-based to being liquid-based, including forced convection, micro-channels; spray and impinging jets; capillary pumped loops; and immersion cooling [3–8]. In the latter, the CPU or circuit board is fully submerged in a stagnant or a flowing dielectric liquid, such as FC-86, FC-72, and HFE-7100.

Dielectric liquids have poor thermo-physical properties and are highly wetting compared with non-dielectric liquids such as water, but they are environmentally friendly and chemically inert. When used in conjunction with structured, porous or micro-porous surfaces the removed power by nucleate boiling of these liquids could be high enough for cooling high power CPU chips and microprocessors. For this application, promising dielectric liquids are those with saturation temperatures <80 °C in order to keep the junction temperature <85–100 °C. However, since liquids, such as the Fluorinert FC-72, are highly wetting (surface tension of 0.008 N/m at room temperature compared to 0.072 N/m for water) air for promoting bubble nucleation is entrapped only in the tiny pores and cavities on the surface. As a result, boiling incipience is delayed until after reaching high surface superheats that could exceed 35 K [3,6,9–11], referred to as temperature excursion. Because such excursions occur at relatively low heat fluxes that CPUs chips are likely to operate at in actual devices for extended periods of time, they could reduce the lifetime and increase the failure frequency of these devices [12].

Enhancements in nucleate boiling are realized through an increase in the density of active nucleation sites on the surface and/or in the detaching frequency of the bubbles. Decreasing the bubbles departure diameter increases this frequency and increasing the nucleation sites density decreases surface superheat and increases nucleate boiling heat flux [13,14]. The very low surface tension of dielectric liquids decreases the detaching diameter of bubbles and increases their departure frequency [10,15]. Recently, Ramaswamy et al. [15] measured an average detachment diameter of FC-72 bubbles from a structured porous surface of ~0.5–0.7 mm at frequencies of 150–200 s^{-1}, depending on the wall superheat. In pool boiling of HFE-7100 on smooth copper the reported average diameter of detaching bubbles is ~0.55 mm at a frequency of 100 s^{-1} [10,11]. Increasing the active nucleation sites density has been attempted using roughened surfaces [16], surfaces with re-entrant cavities [17,18], structured surfaces [15], porous metallic coatings, with average size particles from a few to tens of microns [19], micro-porous coatings, with an average particle sizes of 1–20 μm [3,20–23], and micro-finned silicon surfaces [24,25]. Generally, these surfaces increased nucleate boiling heat transfer coefficient and critical heat flux (CHF), decreased surface superheat, and reduced, and in some cases eliminated, temperature excursion at boiling incipience. As indicated later the porous graphite used in the present experiments has tiny pores and relatively large re-entrant cavities, thus reviewing the reported work on pool boiling of FC-72 on porous and micro-porous surfaces and those with re-entrant cavities is relevant.

Baldwin et al. [17] investigated saturation boiling of FC-72 on surfaces with bulb- and pyramidal-shaped re-entrant cavities with center-to-center spacing of 0.5, 1.0, and 1.5 mm and average round mouths of 45 μm^2. The reported CHF of ~40 W/cm^2 on the surface with pyramidal-shaped re-entrant cavities is 15% higher and

the corresponding surface superheat of ~35 K is 40% lower than those measured on the surface with bulb-shaped cavities. This CHF is also much higher than those reported on smooth surfaces (~13–16 W/cm^2) [20,22,26,27]. Kubo et al. [18] investigated nucleate boiling of 3 and 25 K subcooled FC-72 on smooth silicon and on silicon with re-entrant cavities. These cavities with average mouth diameters of 1.6 and 3.1 μm were spaced by 1.0 and 0.1 mm and had number densities of 81 and 9.3×10^3 cm^{-2}, respectively. Both the nucleate boiling heat transfer coefficient and CHF increased with the best results are those of the surface with the large mouth and high number density cavities. Saturation nucleate boiling ensued at a surface superheat of ~4.8 K, compared to ~15 K on smooth silicon. At 25 K subcooling the reported CHF was ~37% higher and the corresponding surface superheat was ~47% lower than on smooth silicon.

Arbelaez et al. [28] investigated saturated boiling of FC-72 on aluminum foam measuring $2.54 \times 6.35 \times 6.35$ cm and that has porosities of 90–98% and 5–40 pores per linear inch. The surface superheats at boiling incipience were 8–10 K with no temperature excursion, except in two cases it was ~2 K. The nucleate boiling heat flux was ~5 times higher and CHF (28.8 W/cm^2) was ~50% higher than those measured on a machined aluminum block measuring $1.0 \times 2.5 \times 2.5$ cm, however, the surface superheat at CHF on the foam was ~40 K higher. Honda et al. [24] investigated saturation and subcooled (3, 25, and 45 K) boiling of FC-72 on smooth silicon and on silicon sputtered with SiO_2 and chemically etched to a RMS roughness of 25–32 nm. The temperature excursions at boiling incipience on smooth silicon was as much as 37 K, but only ~10 K on the roughened surface, which may be attributed to the trapped air in the surface features. In addition to the enhancement in nucleate boiling heat transfer coefficient, CHF was ~40% higher than that on smooth Si. Rainey and You [3] have reported similar enhancements for FC-72 on a machine roughened copper surface. The temperature excursions at boiling incipience were lower and CHF (18.8 W/cm^2) was ~40% higher than that on polished Cu (13.2 W/cm^2). In saturation boiling of FC-72 on commercially available structured surfaces (Union Carbide's High Flux, Hitachi's Thermoexel-E, and Wieland's Gewa-T) Marto and Lepere [29] have reported 2–5 times higher nucleate boiling heat flux and lower temperatures at boiling incipience than on plain copper, but little or no enhancement in CHF. In the same investigation but with a Turbo-B surface a 91% increase in CHF was reported.

Many saturation and subcooled boiling experiments of FC-72 on micro-porous coatings have shown very promising results, which are attributed to the tiny pores in the micro-porous coatings that could range in size from 0.1 to 1 μm [3,21]. These coatings made with 1–20 μm particles bonded with epoxy have low effective thermal conductivity of only ~0.95 W/m K, which could increase the surface temperature. With thin layers of these coatings (~50 μm) applied to flat surfaces and wires, significant enhancements in the nucleate boiling heat transfer coefficient of FC-72 and decreases in temperature excursions at incipient boiling have been reported [3,20–22]. These results are attributed to the increase in nucleation sites and to the ability to entrap air in the micro-pores of the coatings. In saturation boiling of FC-72 on a micro-porous paint, O'Connor et al. [23] reported ~330% increase in nucleate boiling heat flux and ~100% increase in CHF, compared to untreated copper surfaces. Increases of ~33% in the nucleate boiling heat flux and ~100% increase in CHF of FC-72 on micro-porous coatings, compared to untreated copper, have also been reported [22].

Honda and coworkers [24,25] have investigated pool boiling of FC-72 on micro-finned silicon, indicating large enhancements in both the nucleate boiling heat transfer coefficient and CHF. Surface superheat at CHF was smaller than reported by other investigators on structured and porous surfaces and on micro-porous coatings. In an attempt to reduce or eliminate temperature excursions at boiling incipience, several investigators saturated the FC-72 liquid with dissolved air prior to conducting boiling experiments [21,25,30,31]. The presence of dissolved air in the nucleating bubbles has the effect of reducing the vapor pressure and hence, the surface temperature at boiling incipience. With pre-gassed liquid, measurable decreases in temperature excursions at boiling incipience and increases in the low surface superheat nucleate boiling heat flux have been reported. At higher surface superheats, however, the increase in nucleate boiling heat flux gradually diminished before reaching CHF. These results were generally true for both smooth and enhanced surfaces [21,25,31] and have shown that the combination of pre-gassed liquid and structured, porous or micro-porous surfaces could eliminate temperature excursions at boiling incipience.

El-Genk and Parker [6,32] have reported large increases in the nucleate boiling heat transfer coefficient and CHF of HFE-7100 dielectric liquid on porous graphite and no temperature excursion at boiling incipience. However, because of the difference in properties between HFE-7100 and FC-72, the magnitudes of the enhancements and effect of liquid subcooling could be different, which are the focus of this paper. The reported results on CHF of dielectric liquids such as FC-72 and HFE-7100 have shown a linear increase with increased subcooling, however, the value of the rate constant (or subcooling coefficient) depends on the surface characteristics and properties of boiling liquid [6,11,21,23,25,27]. Generally, porous graphite, micro-porous coatings and surfaces with micro-fins resulted in much higher rate

constants than smooth copper and silicon, and roughed SiO_2 surface; more on that later.

This work investigated saturation and subcooled boiling of FC-72 on a porous graphite surface measuring 10 mm × 10 mm and on a smooth copper of the same dimensions for comparison. Digital photographs of boiling on both surfaces at similar heat fluxes are recorded to help explain and interpret the experimental measurements. The CHF values reported by other investigators for FC-72 on Cu, Si, etched SiO_2, and micro-finned silicon surfaces and on micro-porous coatings are compared with present values on both smooth copper and porous graphite. The porous graphite [6,32] is commercially available, structurally strong, and has high thermal conductivity (245 W/m K out of plane and 70 W/m K in plane) and high volume porosity of 60% with 95% of the contained pores and re-entrant type cavities, which are interconnected. In addition to very tiny pores (<1 μm), the re-entrant cavities at the porous graphite surface have mouth sizes that range from a few to hundreds of microns (Fig. 1), increasing the active nucleation sites density and the effective surface area.

2. Test section and experimental procedures

Detailed descriptions of the experimental facility (Fig. 2) and construction and assembly of the test section (Fig. 3) are available elsewhere [6,10,11,32]. As shown in Fig. 2, the test vessel, partially filled with the FC-72 liquid, is placed inside a heated water bath tank. The immersed electric heater at the bottom of the tank helps maintain constant bath temperature, and together with the submerged water cooled coils in the FC-72 liquid, keeps the pool temperature at the desired values in subcooled boiling experiments, to within ±0.5 K. The magnetic stirrer at the bottom of the FC-72 pool speeds the liquid out-gassing and ensures uniform pool temperature prior to conducting the experiments. Owing to the high solubility of air in FC-72, it typically takes a few hours of boiling to outgas the FC-72 liquid in the test vessel prior to conducting the experiments. However, air apparently remains trapped in the tiny pores and surface re-entrant cavities of the porous graphite. Because of the very low surface tension of FC-72, the test vessel is tightly sealed to prevent liquid leakage. The water-cooled reflux condenser coil on the inside of the cover plate of the vessel (Fig. 2) effectively condenses the generated vapor, thus maintaining constant liquid pool height in the experiments. The FC-72 pool temperature is monitored using four submerged K-type thermocouples and taken as the average of those indicated by the two thermocouples placed a few millimeters from the porous graphite or copper surface.

2.1. Test section

The porous graphite used in this work has highly porous structure with randomly sized interconnected pores and cavities that vary in sizes from <1 μm to tens and hundreds in microns. Re-entrant cavities at the surface have non-circular openings and ragged non-smooth interior and could be several hundred microns deep (Fig. 1). The high volume porosity of the graphite entraps air, even after the degassing the liquid pool, for a long time in many subsequent experiments conducted without opening the test vessel. The graphite block measures 10 × 10 mm in surface area and is 3.0 mm thick (Fig. 3a) and the test section consists of a Teflon block with a square cavity at the center of top surface for placing the heating element below the porous graphite or smooth copper block; the latter has the same surface area (10 × 10 mm) and is 1.6 mm thick. The porous graphite and the smooth copper blocks are mounted onto the heating element using a thin layer of epoxy (~0.1 mm) that has high thermal conductivity and high electrical resistivity (Fig. 3a and b). Two copper leads ~0.5 mm in diameter are soldered to the ends of the Nichrome wire of the heating element to reduce electrical losses. Two K-type thermocouples are inserted in two 0.6 mm diameter horizontal holes on one side, ~0.8 mm from the surface and half way into the graphite or the copper block for monitoring the surface temperature in the experiments (Fig. 3a and b). The average reading of these thermocouples is taken as the surface temperature for the purpose of constructing the pool boiling curves. The estimated temperature drop in the experiments between the surface and the embedded thermocouples in the porous graphite and copper blocks is ⩽1.0 and 0.5 K, respectively.

The test section is encased in a Lexan frame with a closed bottom (Fig. 3) and the shallow cavity on top is filled with translucent two-part epoxy adhesive that also seals the sides of the porous graphite and copper blocks (Fig. 3) to prevent the formation of any tiny grooves that could act as active nucleation sites for vapor bubbles in the experiments, thus skewing the pool boiling curves. Prior to conducting the experiments with copper, its surface is prepared using consistent procedures. It is sanded with emery paper #400 in even strokes to remove scratches and dents, then polished with a metal polishing liquid and cleansed with water and alcohol, and finally finished using fine emery paper (#1500).

2.2. Experimental procedures

The fully assembled and instrumented test section (Fig. 3) is immersed in the FC-72 liquid pool in the test vessel with the surface of the porous graphite or smooth copper is ~8 cm below the free surface of the liquid

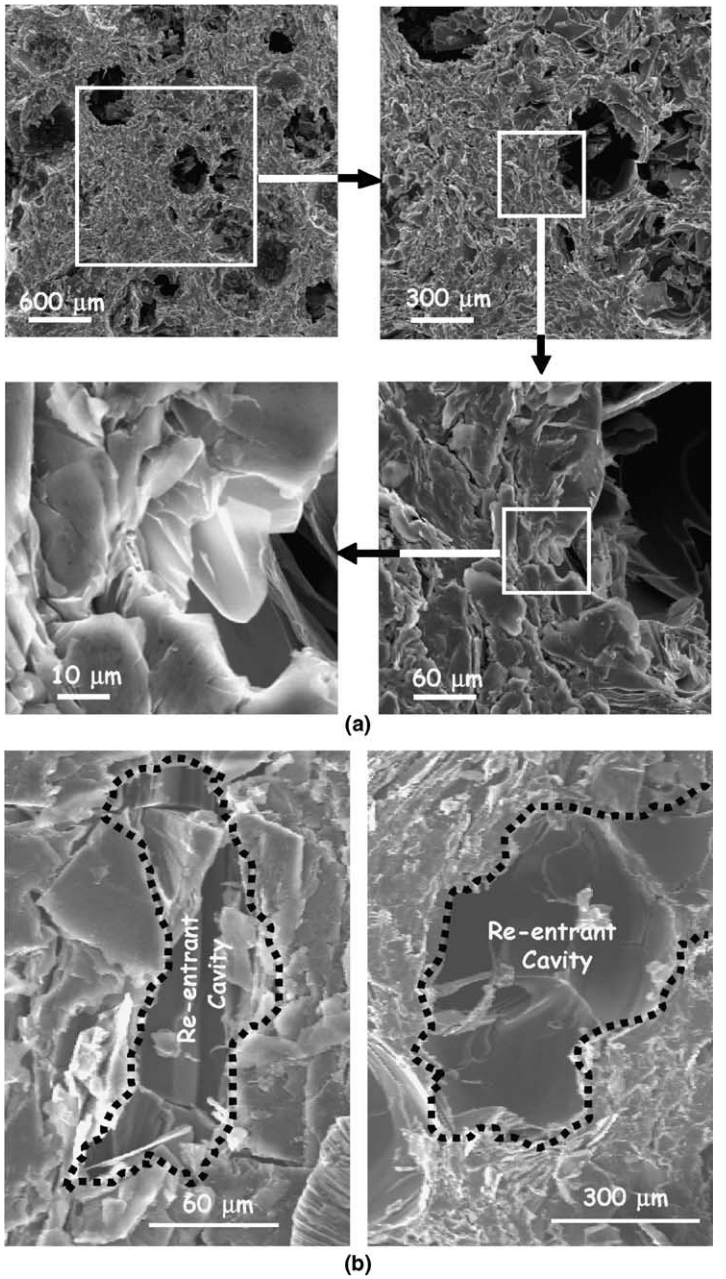

Fig. 1. Scanning electron microscope (SEM) images of the porous graphite surface. (a) Porous graphite surface at different magnification and (b) re-entrant surface cavities.

pool. Out-gassing the liquid pool is accomplished by boiling it for several hours while maintaining the temperature of the surrounding water bath (Fig. 2) a few degrees above the saturation temperature of FC-72 and turning the magnetic stirrer at the bottom of the pool on (Fig. 2). The released gas is intermittently vented out of the test vessel using the valve in the cover plate of the vessel (Fig. 2). In subcooled boiling, the temperature of the water bath is kept close to the desired pool temperature and the immersed water-cooled coils in the pool kept the temperature of the FC-72 liquid constant to within <1.0 K throughout the entire experiments. In these experiments, no air is allowed to enter the test vessel prior to or during the test procedures, thus the effective vapor pressure is that corresponding to the liquid subcooling in the pool.

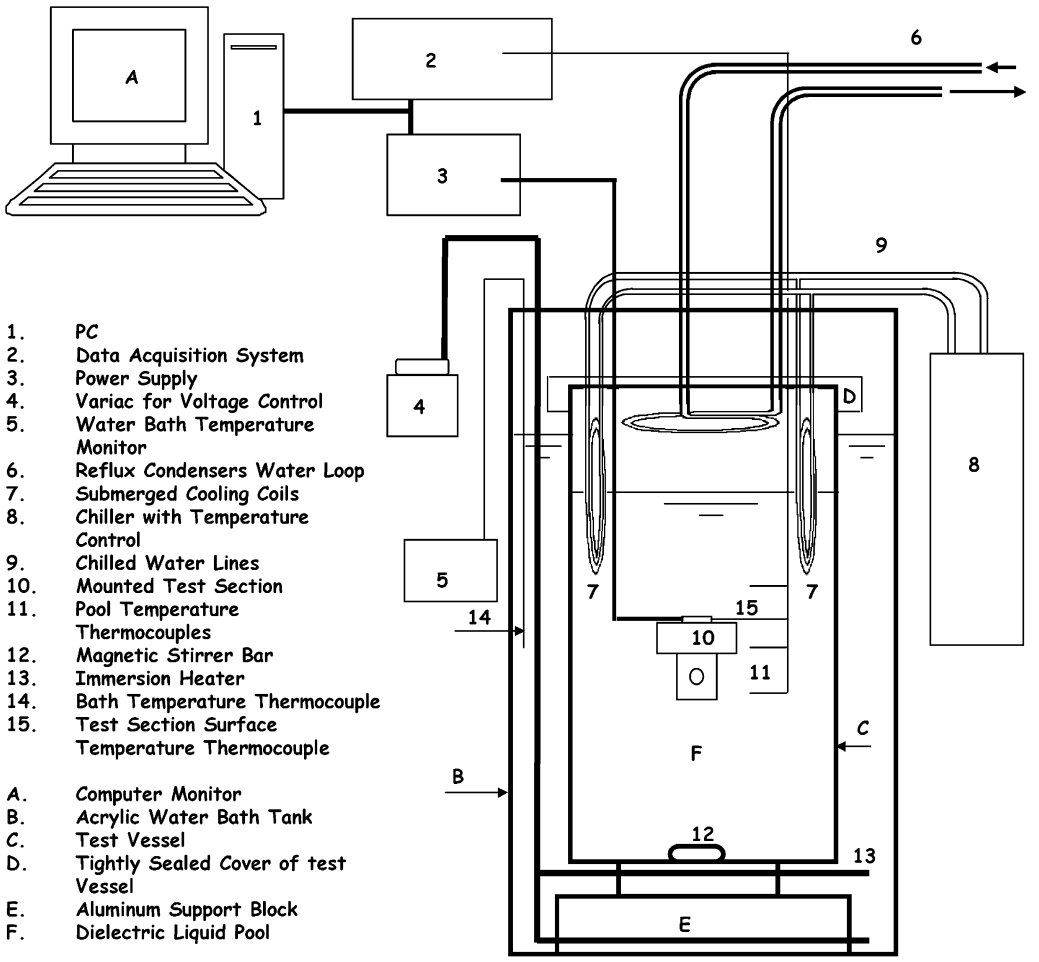

Fig. 2. Line diagram of the pool boiling test facility.

After the out-gassing of the liquid pool is complete, experiments began by turning off the magnetic stirrer at the bottom of the test vessel and incrementally increasing the electrical power to the heating element in the test section, via increasing the applied voltage in increments of $\leqslant$0.2 V. The measured voltage drop across and current through the heating element determine the dissipating heat flux from the boiling surface (Fig. 2). The side heat losses from the assembled test section are found to be negligibly small [10,11], based of a thermal analysis of the section using ANSYS commercial finite element software [10,11]. Following each incremental increase in the dissipated power by the heating element, the surface heat flux and temperature are recorded after reaching steady state condition; when two successive measurements of the surface temperature are within ±0.2 K. Each of these measurements is the average of 30 subsequent readings by the two thermocouples embedded in the graphite or copper block (Fig. 3). It took typically ~45–60 seconds after incrementally increasing the heater's power to reach steady state. When either thermocouples in the graphite or copper block (Fig. 3) measured an rapid increase in temperature of >30 K above the last steady state measurement, it is considered an indication of reaching the critical heat flux (CHF) and the experiment was terminated. The estimated experimental uncertainties are ±0.7 K in temperature and ±2% in surface heat flux measurements.

3. Results and discussion

The obtained curves for saturation and 10, 20, and 30 K subcooled boiling FC-72 liquid on porous graphite in two sequential tests conducted at the same conditions are shown in Fig. 4a–d, respectively; the solid square symbols indicate CHF. In addition to the excellent reproducibility, these figures show higher nucleate boiling heat fluxes and CHF for FC-72 on porous graphite than on copper.

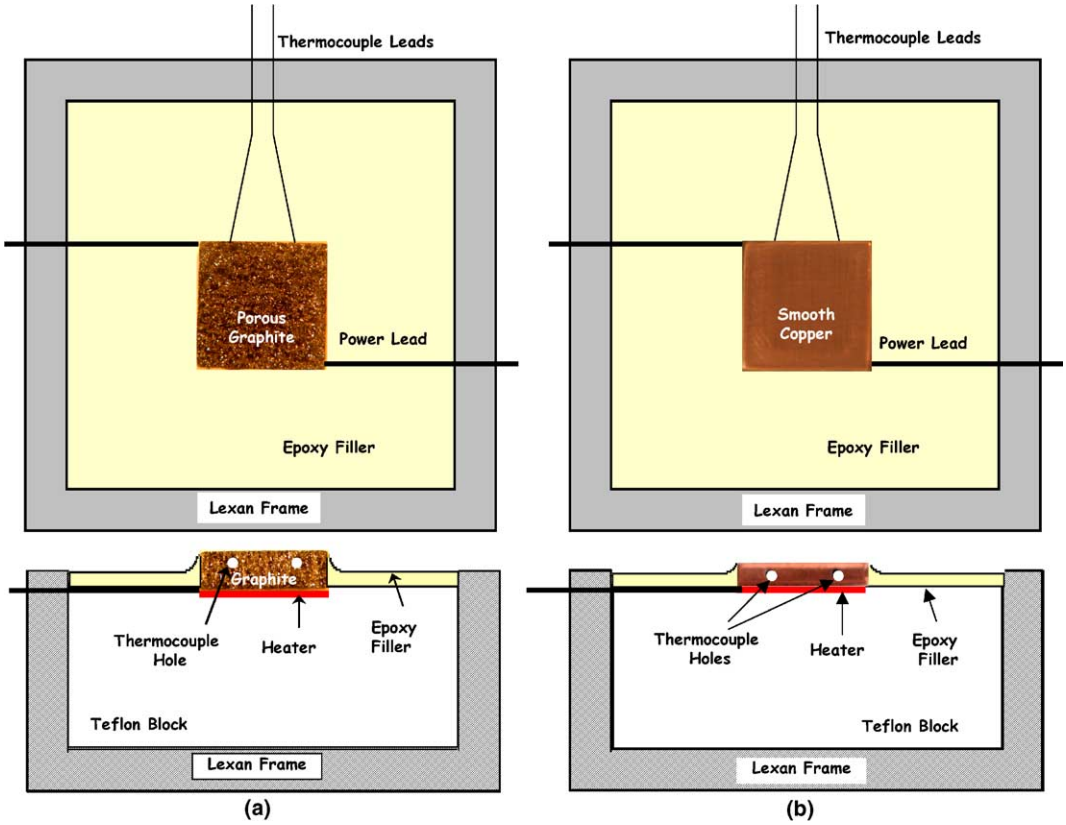

Fig. 3. Cross-sectional views and photographs of assembled test sections. (a) Porous graphite test section and (b) smooth copper test section.

3.1. Comparison of boiling curves on porous graphite and smooth copper

The obtained boiling curves for FC-72 on porous graphite and smooth copper are compared in Fig. 5a–d. These figures show no temperature excursions at boiling incipience on porous graphite on which nucleate boiling ensues when surface temperature is <1.0 K above saturation temperature of FC-72 (because of high elevation of Albuquerque, NM, ambient pressure is ~0.086 MPa and saturation temperature is ~52 °C). Conversely, the temperature excursions prior to boiling incipience on copper varied from 9.0 to 14 K, depending on the liquid subcooling (Fig. 5a–d). The absence of temperature excursions prior to boiling incipience on porous graphite is attributed to the air entrapped in the tiny and interconnected pores and re-entrant cavities at the surface. Because of the low surface tension of FC-72, pores with mouth sizes <12.8 μm would not be readily wetted, thus entrapping air (Fig. 1a). The larger pores and re-entrant cavities, however, are likely filled with liquid, but some of the interconnecting pores to these cavities could be too small to be wetted, thus entrap air (Fig. 1b).

Tiny bubbles that likely contain some of the air entrapped in the tiny pores and re-entrant cavities in the porous graphite are seen released from the surface in subcooled boiling experiments when the measured surface temperature is higher than that of the liquid pool but well below the saturation temperature of FC-72. Conversely, no such bubbles are released from the copper surface in the natural convection regime prior to boiling incipience because only a meager amount of air is entrapped in the crevices of the copper surface owing to the low surface tension of FC-72.

Noteworthy are the significant increases in the nucleate boiling heat transfer coefficient (high nucleate boiling heat flux and low surface superheat) and CHF of FC-72 on porous graphite compared to those on copper (Fig. 5a–d). Also, boiling incipience on porous graphite occurred at very low surface superheats ($\Delta T_{sat} < 1.0$ K), while at boiling incipience on copper ΔT_{sat} varied from 5.5 to 8.8 K. The measured saturation CHF on porous graphite (27.3 W/cm^2) is ~60% higher than that on Cu (16.9 W/cm^2) and occurs at $\Delta T_{sat} = 12$ K versus 21 K on copper. Similar enhancements at $\Delta T_{sub} = 10$, 20, and 30 K are obtained and shown in Fig. 5b–d, respectively. The measured CHF values of 39.6, 49.0, and

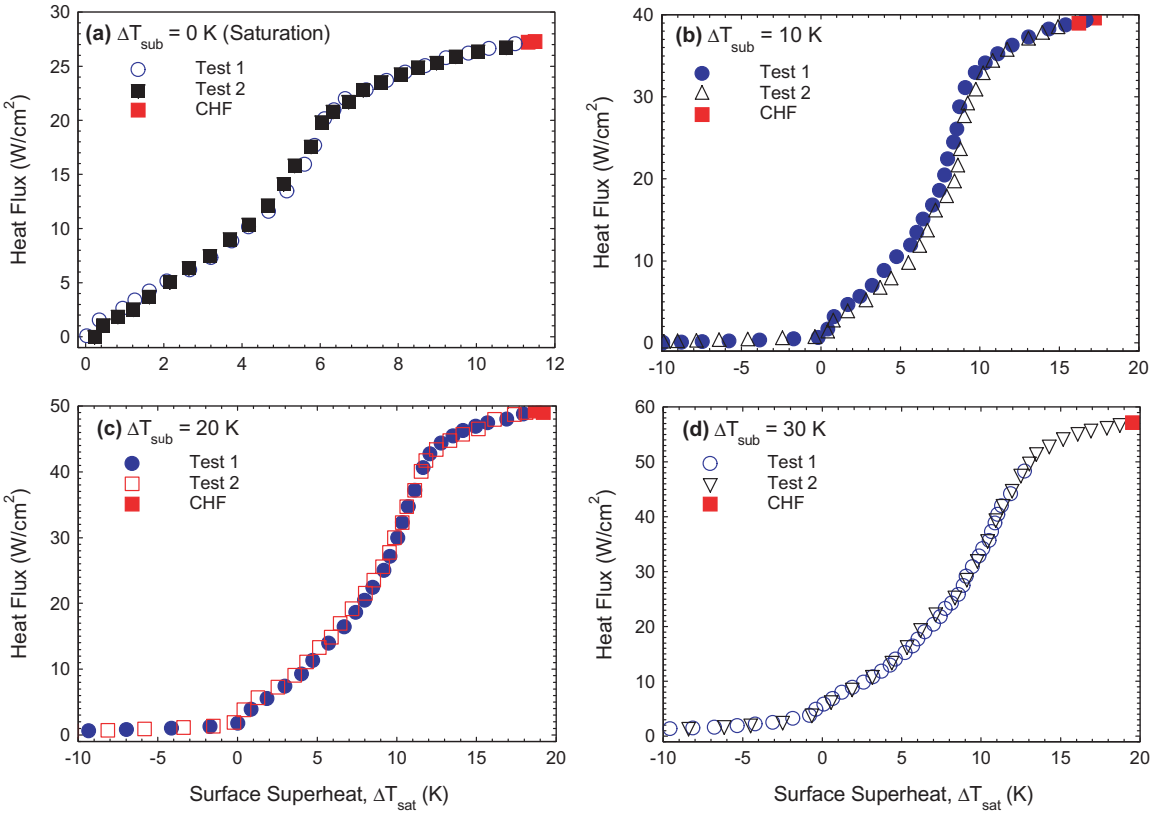

Fig. 4. Boiling curves for saturation and subcooled boiling of FC-72 on porous graphite.

57.1 W/cm^2 at 10, 20, and 30 subcooling, respectively, represent increases of ~81%, 82%, and 94%, respectively, over those on smooth copper. The surface superheat at CHF, $\Delta T_{sat,CHF}$, on porous graphite is 11.8 K in saturation boiling and increases with increased liquid subcooling to 19.5 K when $\Delta T_{sub} = 30$ K. On copper, $\Delta T_{sat,CHF}$ is much higher; 21.3 K in saturation boiling and 24.9 K when $\Delta T_{sub} = 30$ K (Fig. 5b–d).

3.2. Nucleate boiling regimes

Fig. 6a–c present the saturation and subcooled boiling curves of FC-72 on porous graphite, while Fig. 6d–f present the obtained boiling curves on smooth copper. The horizontal arrows labeled "NC" indicate the extent of the natural convection region, prior to boiling incipience. Fig. 6a–c indicate the absence of temperature excursion prior to boiling incipience on porous graphite, while Fig. 6d–f show these excursions on copper to decrease from 14 K in saturation boiling to 13.5, 10, and 9 K at $\Delta T_{sub} = 10$, 20, and 30 K, respectively. Reported results by other investigators for dielectric liquids have indicated much higher temperature excursions prior to boiling incipience than those measured in this work on Cu [6,9–11,22,23].

In addition to the natural convection region the boiling curves of FC-72 on porous graphite and copper have three distinct nucleate boiling Regions I, II, and III. On porous graphite natural convection only exists in subcooled boiling (Fig. 6a–c), but on copper it exists in saturation as well as subcooled boiling (Fig. 6d–f). The obtained data in the natural convection region are presented and discussed in the next section. Region I is that of low-superheat nucleate boiling. On porous graphite it begins when the surface temperature is only slightly higher than saturation ($\Delta T_{sat} < 1.0$ K) and experiences a significant increase in the number of discrete bubbles departing from the surface and an increase in the nucleate boiling heat transfer coefficient with increasing ΔT_{sat} (Fig. 6b and c). In Region II, the slopes of the pool boiling curves and the number of discrete bubbles departing from the surface are much higher than in Region I, increasing the rate of increasing the nucleate boiling heat transfer coefficient (or heat flux) with increased ΔT_{sat}. Such an increase is indicative of the increase in the active nucleation sites density on the surface and hence, the number of departing bubbles with increasing surface temperature or superheat.

As the number of departing bubbles increases, bubbles begin to coalesce forming vapor globules near the

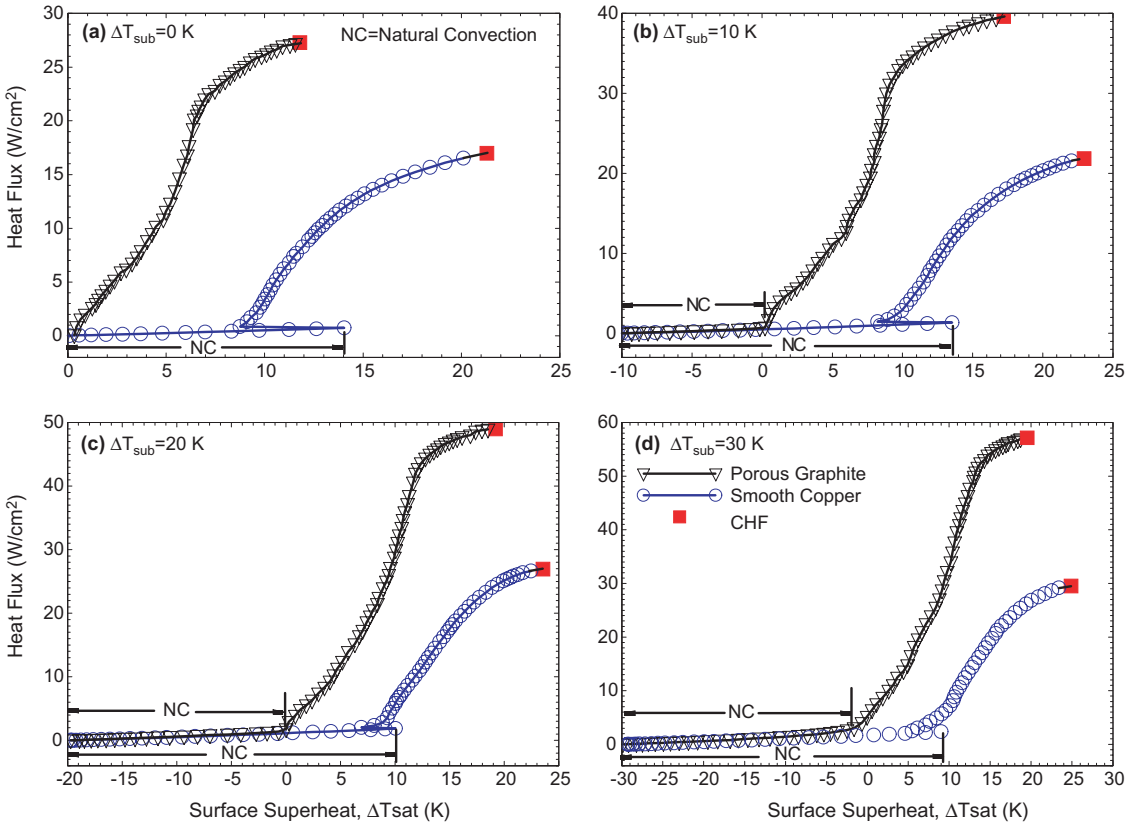

Fig. 5. Comparisons of boiling curves of FC-72 on porous graphite and copper.

boiling surface, marking the nucleate boiling transitions to Region III. In this region, although the density of active nucleation sites and the number of departing bubbles continue to increase with increased surface heat flux, the coalescence of these bubbles into vapor globules results in a large increase in surface temperature with increasing heat flux or a decrease in the heat transfer coefficient with increased surface superheat. Consequently, the increase in the nucleate boiling heat flux in Region III with increasing surface superheat is significantly lower than in Regions II and I. Region III ends when reaching CHF, marked by a solid square symbol in Fig. 6a–f. These figures show CHF and corresponding surface superheat, $\Delta T_{sat,CHF}$, increase with increased liquid subcooling; more details on that are presented in a later section.

3.3. Natural convection region

Natural convection of FC-72 on porous graphite only occurs in subcooled boiling, when the surface temperature is higher than that of the bulk liquid but below its saturation temperature ($T_b \leqslant T_w \leqslant T_{sat}$) and the natural convention region extents to boiling incipience, when the surface temperature is <1.0 K above saturation (Fig. 6b–d). On copper, natural convection occurs both in saturation and subcooled boiling and extends to the end of the temperature excursion prior to boiling incipience (Fig. 6e and f). In the experiments, since the porous graphite and the copper surfaces are uniformly heated the dissipated heat flux in the natural convection region is proportional to $(T_w - T_b)^{1.2}$ (Fig. 7a and b). The present natural convection heat transfer data for FC-72, earlier data for HFE-7100 [32] on porous graphite and copper, and the reported data by other investigators for FC-72 on micro-porous coatings and on surfaces with micro-fines and micro-reentrant cavities [18,20,21] are shown and correlated in Fig. 7a and b as

$$q_{NC} = 0.0353(T_w - T_b)^{1.2},$$
on porous and structured surfaces (Fig. 7a), and
$$q_{NC} = 0.0314(T_w - T_b)^{1.2},$$
on smooth surfaces (Fig. 7b). (1)

These correlations fit the data in Fig. 7a and b to within ±10% and ±7%, respectively, indicating that the natural convection heat transfer coefficient for the dielectric liquids FC-72 and HFE-7100 on porous and structured

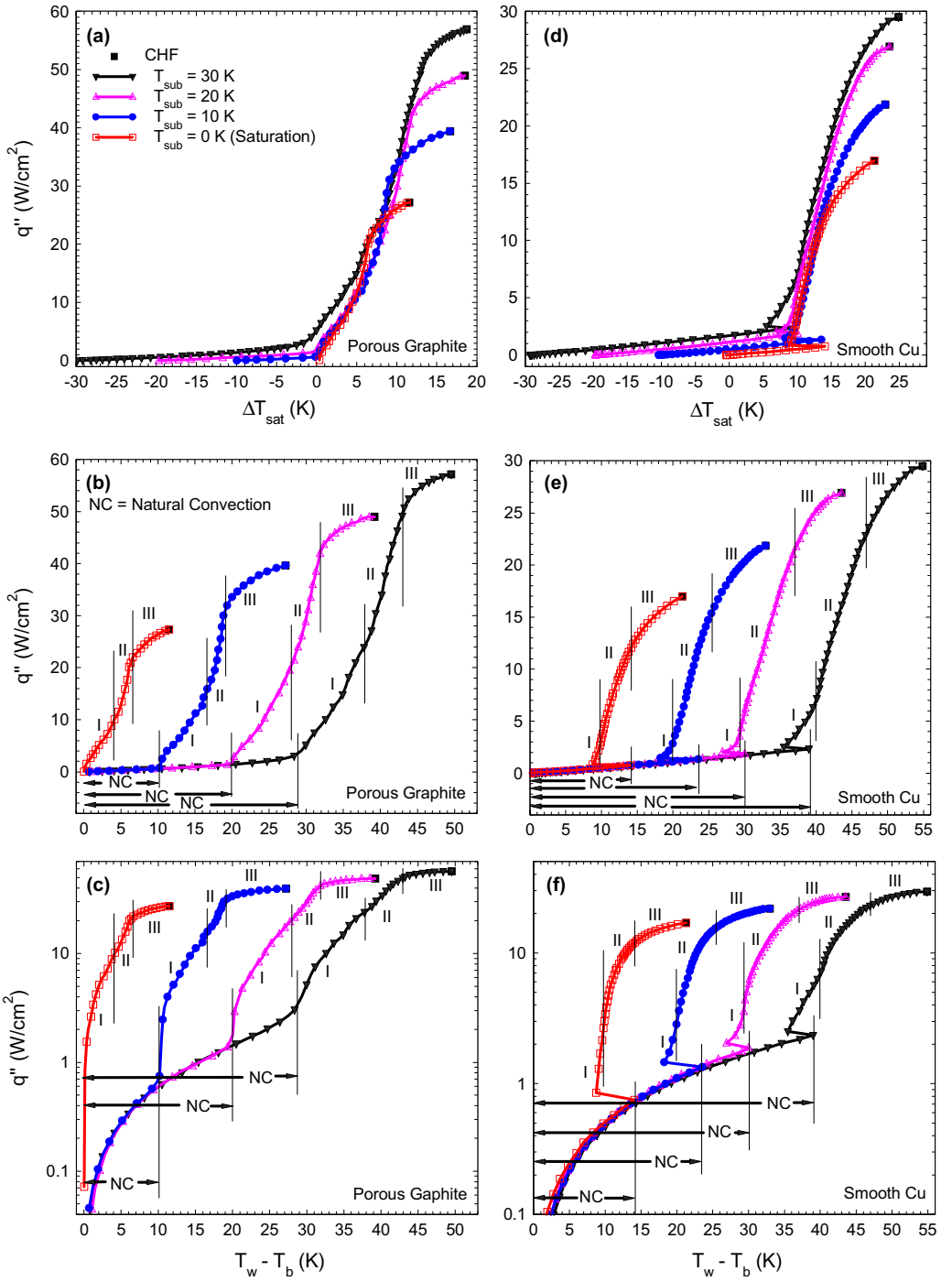

Fig. 6. Saturation and subcooled boiling curves on porous graphite and copper.

surfaces is ~12.4% higher than on smooth copper. The enhancement in natural convention of FC-72 on porous graphite (~19%) compared to that on copper [32], is attributed to the induced mixing in the thermal boundary layer by the released tiny bubbles of vapor and dissolved air from the surface, when its temperature was below the saturation temperature of the liquid. This may also explain the consistency of the present natural

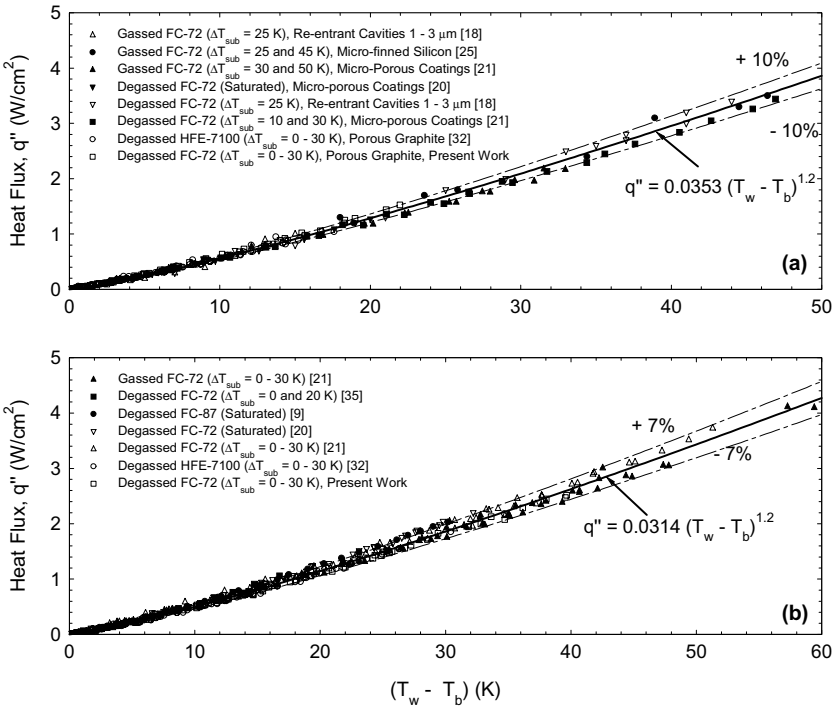

Fig. 7. Natural convection data of FC-72 liquid on smooth surfaces and porous, micro-porous, and structures surfaces. (a) Porous and structured surface and (b) copper and silicon.

convection data on porous graphite with that reported on micro-porous and structured surfaces from which bubbles of vapor and dissolved air could have also been released prior to boiling incipience. On the other hand, no such bubbles are released from the copper surface in the natural convection region and prior to boiling incipience (Fig. 7b).

3.4. Nucleate boiling heat transfer

Fig. 5a–d clearly show that the nucleate boiling heat transfer coefficients on porous graphite are significantly higher than on Cu. At $\Delta T_{sat} = 10$ K the saturation nucleate heat flux on porous graphite is 26.2 W/cm^2, compared to only 3.3 W/cm^2 on copper. Also, at the same nucleate boiling heat fluxes of 5 and 15 W/cm^2 the corresponding surface superheats are 2.2 and 5.7 K on the porous graphite compared to 10.5 and 17.3 K on copper (Fig. 5a). Similar enhancements occurred in subcooled nucleate boiling of FC-72 on porous graphite (Figs. 5 and 6). Table 1 lists CHF and $\Delta T_{sat,CHF}$ and some saturation and subcooled nucleate boiling heat fluxes and the corresponding surface superheats and heat transfer coefficients for FC-72 on porous graphite and on copper.

Table 1
Comparison of boiling data for FC-72 on porous graphite and smooth copper

Parameter	Porous graphite				Smooth copper			
	Sat., $\Delta T_{sub} = 0$ K	10 K	20 K	30 K	Sat., $\Delta T_{sub} = 0$ K	10 K	20 K	30 K
$\Delta T_{sat,ex}$ (K)	None	None	None	None	14.0	13.5	10.0	9.0
$\Delta T_{sat,i}$ (K)	$\leqslant$0.5	$\leqslant$0.5	$\leqslant$0.5	$\leqslant$0.5	$\leqslant$8.8	$\leqslant$8.2	$\leqslant$6.9	$\leqslant$5.5
CHF (W/cm^2)	27.3	39.6	49.0	57.1	16.9	21.9	26.9	29.5
$\Delta T_{sat,CHF}$ (K)	11.8	17.2	19.2	19.5	21.3	22.9	23.5	24.9
q_{NB} (W/cm^2) [HTC (W/cm^2 K)]								
at $\Delta T_{sat} = 11$ K	27.10 [2.46]	35.10 [3.19]	36.80 [3.3]	40.00 [3.64]	6.30 [0.57]	5.20 [0.47]	8.30 [0.75]	9.90 [0.90]
at $\Delta T_{sat} = 14$ K	N/A	38.00 [2.71]	45.90 [3.28]	52.70 [3.76]	11.90 [0.85]	13.00 [0.93]	15.30 [1.09]	17.00 [1.21]
at $\Delta T_{sat} = 17$ K	N/A	39.50 [2.32]	48.10 [2.83]	56.00 [3.29]	14.80 [0.87]	17.50 [1.03]	21.40 [1.26]	23.10 [1.36]

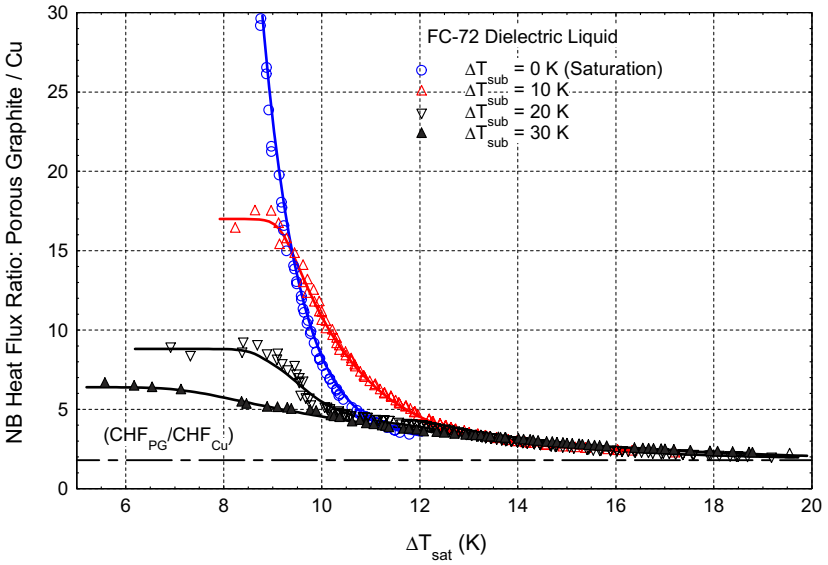

Fig. 8. Nucleate boiling heat flux ratios on porous graphite and copper.

The high heat transfer coefficients and low surface superheats in nucleate boiling of FC-72 liquid on porous graphite translate into high dissipation power and low junction temperatures and, hence, long operation life and low frequency of thermally induced failures of high power computer chips [12]. In addition, the absence of temperature excursions at boiling incipience on porous graphite is an attractive feature for cooling CPU chips at low heat fluxes (<5 W/cm^2) they are expected to operate the longest time.

To quantify the enhancements in nucleate boiling on porous graphite, the ratios of nucleate boiling heat transfer coefficient (NHTC) of FC-72 on porous graphite and copper are plotted in Fig. 8 versus ΔT_{sat}. The data in this figure are obtained from the pool boiling curves in Fig. 5a–d. Fig. 8 shows that at $\Delta T_{sat} \simeq 9$ K, saturation NHTC of FC-72 on porous graphite is ~30 times that on copper, but this ratio decreases exponentially with increased surface superheat approaching an asymptote of ~1.8. This ratio is approximately 13% higher that the saturation critical heat flux ratio ($CHF_{PG}/CHF_{Cu} \sim 1.61$). When $\Delta T_{sub} = 10$ K, the NHTC ratio is constant and equal to 17.0 up to $\Delta T_{sat} = 9.0$ K, and for $\Delta T_{sub} = 20$ K this ratio =8.8 up to $\Delta T_{sat} = 8.5$ K, and =6.4 up to $\Delta T_{sat} = 6.5$ K when $\Delta T_{sub} = 30$ K. Beyond these surface superheats, these ratios of NHTC decrease exponentially with increasing surface superheat, approaching the same asymptote as the saturation nucleate boiling ratio (~1.8) (Fig. 8).

3.5. Critical heat flux

To quantify the increases in CHF for FC-72 with increased liquid subcooling, the CHF ratios (CHF_{PG}/CHF_{Cu}) and those of the corresponding surface superheats ($\Delta T_{sat,PG}/\Delta T_{sat,Cu}$) on porous graphite and copper are plotted versus ΔT_{sub} in Fig. 9a and b, respectively. As indicated earlier and delineated in Fig. 5a–d, CHF values for FC-72 on porous graphite are higher and the corresponding surface superheats are lower than on copper (Table 1). (CHF_{PG}/CHF_{Cu}) increases with increased liquid subcooling from ~1.6 ± 5% in saturation boiling ($\Delta T_{sub} = 0$ K) to 2.1 ± 5% at $\Delta T_{sub} = 30$ K (Fig. 9a), while ($\Delta T_{sat,PG}/\Delta T_{sat,Cu}$) increases with increased liquid subcooling from 0.47 ± 15% in saturation boiling to 0.68 ± 15% when $\Delta T_{sub} = 15$ K, then increases very little to 0.7 ± 15% when $\Delta T_{sub} = 30$ K (Fig. 9b).

Saturation CHF values of FC-72 on porous graphite and on copper are correlated using the form suggested by Kutateladze [33] as

$$CHF_{sat} = C_{CHF,sat}\rho_v^{0.5} h_{fg}[\sigma g(\rho_l - \rho_v)]^{0.25}. \quad (2)$$

In Fig. 10, the values of the coefficient $C_{CHF,sat}$ for FC-72 on porous graphite and on copper are based on measurements of CHF in 9 and 19 sequential tests, respectively. The best least square fit value of $C_{CHF,sat}$ for FC-72 on Cu is 0.166, which agrees to within +6% and −10% with the values obtained from reported CHF data by other investigators on copper and silicon [3,21,24, 26,34,35]. Similarly, the best fit of the present values of $C_{CHF,sat}$ for FC-72 on porous graphite is 0.263 (Fig. 10). This value is 58.4% higher than that on smooth surfaces (0.166) and within +5% and −7% of the values obtained from the reported CHF data by other investigators for FC-72 on micro-porous coatings [3,21,22,34] and micro-finned silicon surfaces [25]. The data in Fig. 10 indicates that on smooth surfaces, ΔT_{sat}

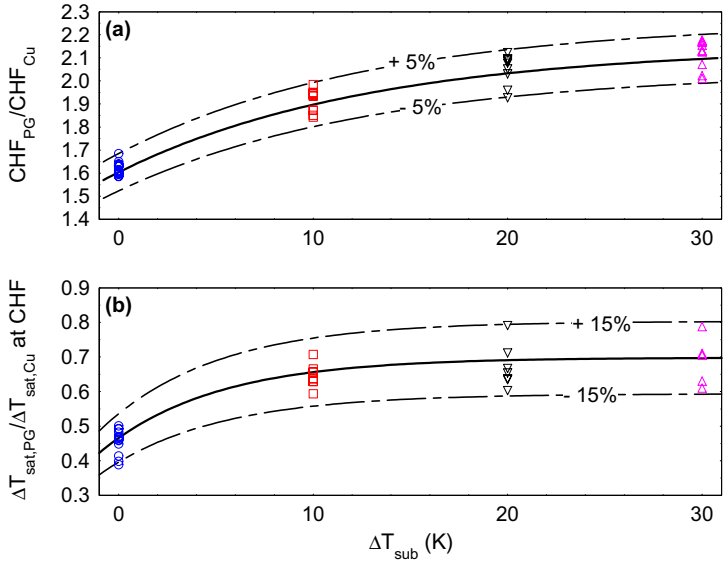

Fig. 9. Enchantment in CHF and decrease in $\Delta T_{sat,CHF}$ for FC-72 on porous graphite.

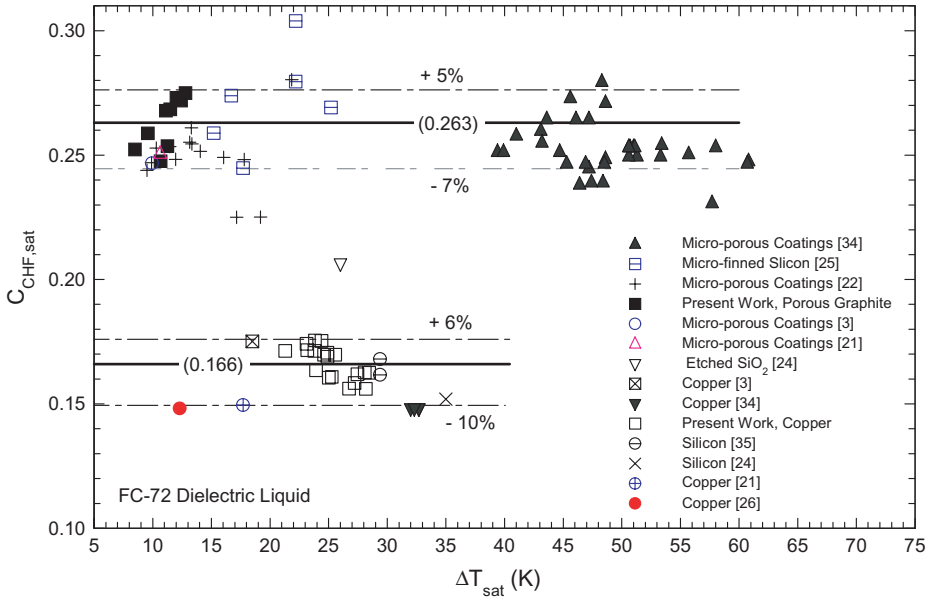

Fig. 10. Comparisons of saturation boiling CHF coefficients for FC-72.

at CHF varies from 12 to 35 K while on porous and micro-porous surfaces it is as little as 8 K to as much as 63 K. The present values of ΔT_{sat} at CHF for FC-72 on copper varied from 21 to 28 K and from 8 to 13 K on porous graphite. The highest surface superheats at CHF are those of O'Connor [34] on micro-porous coatings (39–61 K), which may be attributed to a potential contamination of the FC-72 liquid in the experiments with plasticizers, which have the effect of producing a "tail effect" near CHF.

3.6. Effect of subcooling on CHF

The present values of CHF_{sub} for FC-72 on porous graphite are correlated in terms of CHF_{sat} (Eq. (2)) and ΔT_{sub} using the linear relationship suggested by Ivey

and Morris [36] and used successfully by many investigators [6,11,21,27,32,35] as

$$\mathrm{CHF_{sub}} = \mathrm{CHF_{sat}}(1 + C_{\mathrm{CHF,sub}}\Delta T_{\mathrm{sub}}). \quad (3)$$

The value of the CHF subcooling coefficient, $C_{\mathrm{CHF,sub}}$, determined from the least squares fit of the $\mathrm{CHF_{sub}}$ values at various liquid subcoolings, depends on the characteristics of the surface as well as on the properties of the boiling liquid [6,10,32,36]. For FC-72 on porous graphite, $C_{\mathrm{CHF,sub}} = 0.041$ which make Eq. (3) fit the data to within +5% and −4% (Fig. 11a).

The values of ($\mathrm{CHF_{sub}}/\mathrm{CHF_{sat}}$) obtained from the reported data by a number of investigators for boiling of both gassed and degassed FC-72 liquid on smooth silicon, Cu, and etched SiO_2 surfaces [23–27]; micro-porous coatings [21,23] and micro-finned silicon [24,25] are presented versus ΔT_{sub} in Fig. 11b–d, respectively. For FC-72 on smooth surfaces, including the present data on Cu, $C_{\mathrm{CHF,sub}} = 0.018$, which is within ±6% of the data (Fig. 11b). On micro-porous coatings the values of $C_{\mathrm{CHF,sub}}$ for gassed (0.044) and degassed (0.049) FC-72 liquids are close [21], while that for gassed liquid on micro-porous coating used in [23] is much smaller (0.032) (Fig. 11c). Rainey et al. [21] used micro-porous coatings of aluminum particles, 1–20 μm in size, mixed with epoxy and a solvent, while O'Connor et al. [23] used a micro-porous coating of diamond particles, ranging in size from 8 to 12 μm. Fig. 11d for micro-finned silicon surfaces shows almost no difference in the values of $C_{\mathrm{CHF,sub}}$ for gassed and degassed FC-72 liquids, but rather a strong dependence on surface characteristics. For PF 50–60 surface with 50 μm square and 60 μm high fins [24,25] $C_{\mathrm{CHF,sub}} = 0.022$, but for all other surfaces with different micro-fins dimensions [25] $C_{\mathrm{CHF,sub}}$ (0.036) is ~64% higher.

Fig. 12a compares Eq. (3) for the present data and that reported by various investigators on the effect of liquid subcooling on CHF of FC-72 on smooth, porous, and micro-porous surfaces. As delineated in this figure, the largest increases in CHF with increased subcooling are those measured on micro-porous coatings (4.4%/K and 4.9%/K), followed closely with that measured in the present work on porous graphite (4.1%/K), then micro-fined surfaces (3.6%/K). The smallest increases

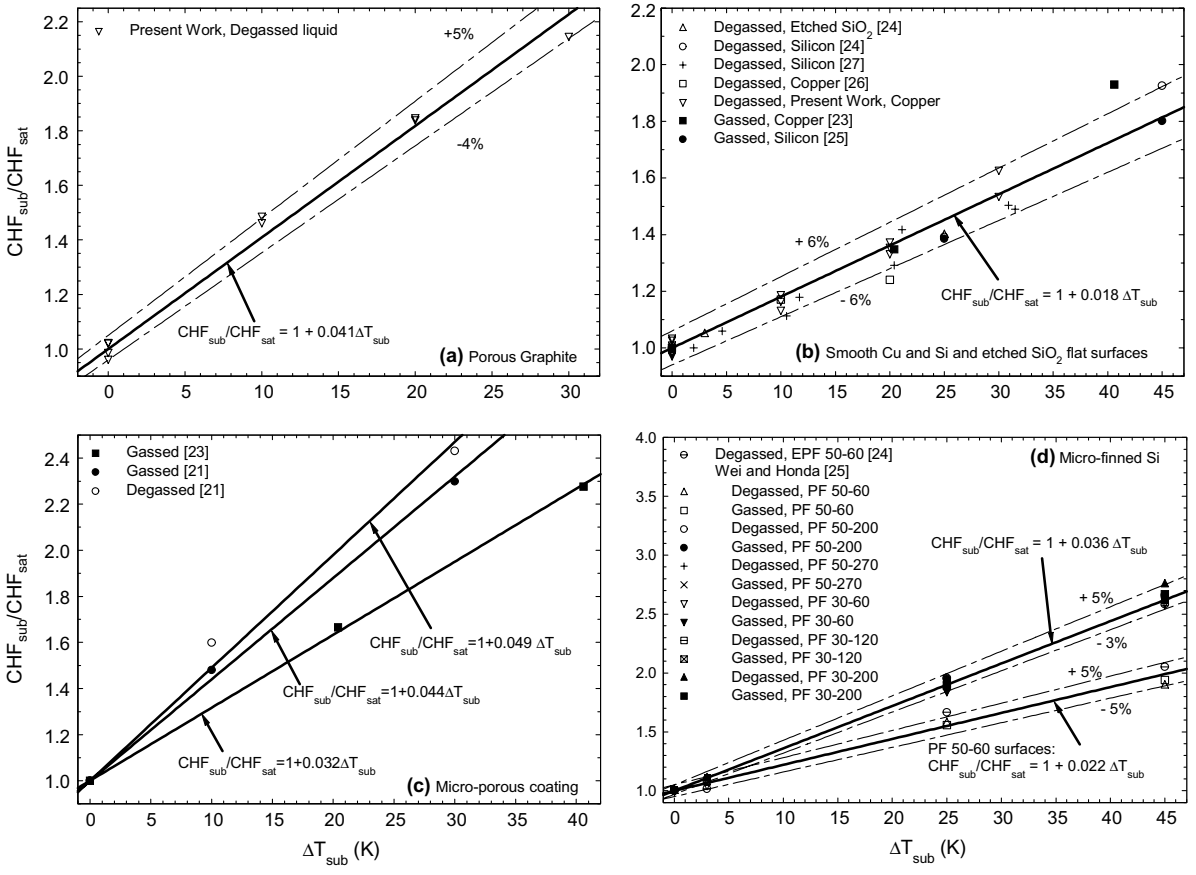

Fig. 11. Effect of subcooling on CHF of FC-72 on PG, smooth surfaces, micro-porous coatings, and micro-finned surfaces.

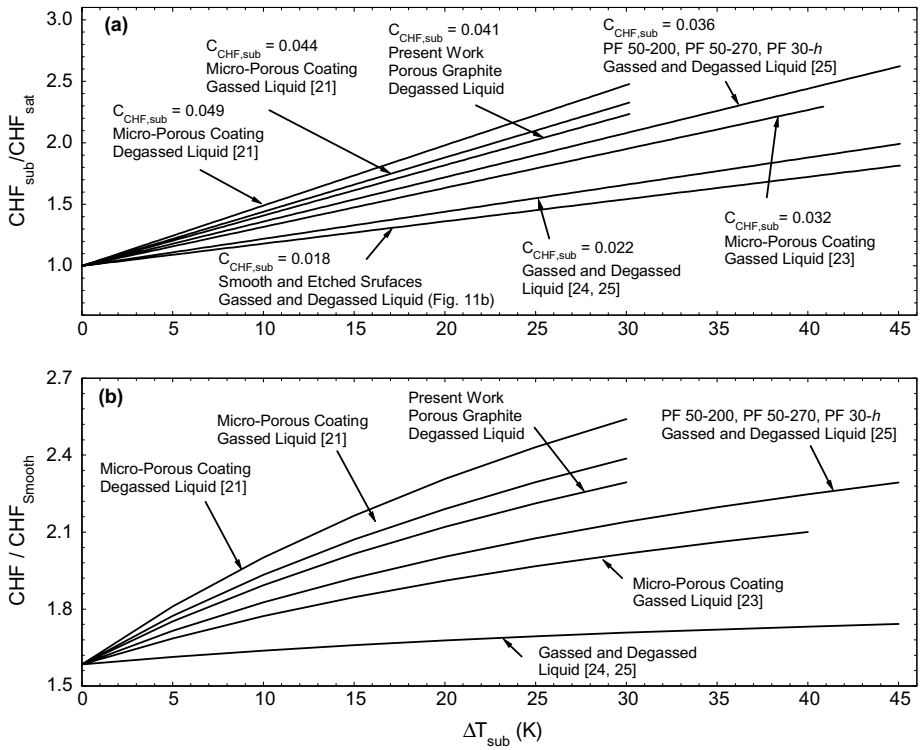

Fig. 12. Summary of subcooling effect and surface enhancement on CHF of FC-72.

are those measured on smooth and etched surfaces (1.8%/K). Fig. 12b compares the enhancement in CHF of FC-72 on porous graphite, micro-porous coatings, and micro-finned surfaces relative to that measured in the present experiments on smooth copper. This figure shows that the largest enhancements in subcooled boiling CHF are those reported for gassed and degassed FC-72 on micro-porous coatings [21], followed by the present values on porous graphite, then those for gassed and degassed liquid on micro-finned surfaces [24,25].

The nucleate boiling photographs presented in Fig. 13 demonstrate higher density of detaching bubbles from the porous graphite surface compared to Cu at almost the same heat fluxes, which is consistent with the measured enhancements in the nucleate boiling heat transfer coefficient and CHF of FC-72 on porous graphite (Fig. 5a–d).

4. Summary and conclusions

Saturation and subcooled boiling of FC-72 liquid on copper and porous graphite surfaces (10×10 mm) are investigated. Porous graphite has a volume porosity of 60%, of which 95% are open and interconnected pores varying in sizes from <1.0 to hundreds of microns. No temperature excursion occurs at boiling incipience on porous graphite, compared to 9.0–14 K on copper. On porous graphite nucleate boiling ensues when $\Delta T_{sat} < 1.0$ K, while on copper boiling incipience occurs at ΔT_{sat} of 5–9 K. Nucleate boiling heat transfer coefficient and CHF on porous graphite are significantly higher and the surface superheats are much lower than on copper. CHF on both Cu and porous graphite increases linearly with increased liquid subcooling, however, the rate of increase (or $C_{CHF,sub}$) on porous graphite is ~125% higher than that on copper, ~20% higher than that on micro-finned silicon surfaces, but slightly lower than that on micro-porous coatings. CHF for FC-72 on porous graphite of 27.3, 39.6, 49.0, and 57.1 W/cm^2 at saturation and at ΔT_{sub} = 10, 20, and 30 K are much higher that those on copper (16.9, 21.9, 26.9, and 29.5 W/cm^2, respectively). The saturation CHF on porous graphite is 1.6 times that on copper and the ratio increases with subcooling to 2.3 at ΔT_{sub} = 30 K. The surface superheat at CHF on porous graphite of 11.8, 17.2, 19.2, and 19.5 K at saturation and 10, 20, and 30 K liquid subcooling are much lower than those on copper (21.3, 22.9, 23.5, and 24.9 K, respectively). The absence of temperature excursions at boiling incipience, the very low surface temperature to ensue boiling, and the high nucleate boiling heat transfer coefficient and CHF of FC-72 on porous graphite demonstrate its

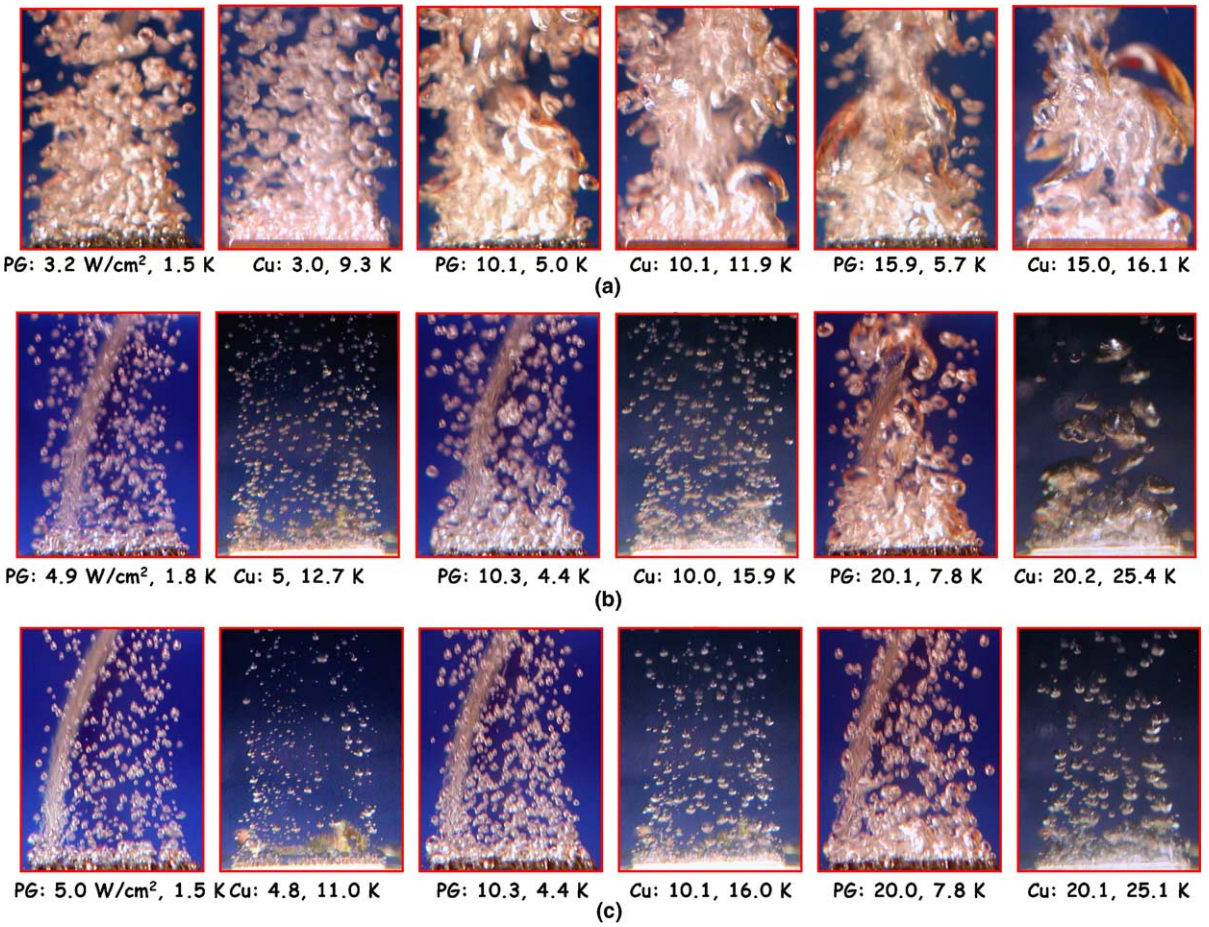

Fig. 13. Photographs of saturation and subcooled nucleate boiling of FC-72 on porous graphite and copper. (a) Saturation boiling, (b) 10 K subcooled boiling and (c) 20 K subcooled boiling.

excellent potential for immersion cooling of CPU chips with average dissipation heat fluxes $\geqslant 55$ W/cm^2. The enhancements in nucleate boiling and CHF on porous graphite are attributed to a high nucleation site density and the entrapped air in multitude of small pores and re-entrant cavities of various sizes at the surface. The latter are responsible for the absence of temperature excursion at boiling incipience at heat fluxes of $\geqslant 2$ W/cm^2. At such heat fluxes, CPU chips are likely to operate for extended periods of time, which translates into long operation life and low failure frequency.

References

[1] G. Xu, B. Guenin, M. Vogel, Extension of air cooling for high power processors, in: Proc. 9th Intersociety Conf. on Thermal Phenomena, vol. 1, 2004, pp. 186–193.

[2] J. Knickerbocker et al., An advanced multichip module (MCM) for high-performance UNIX servers, IBM J. Res. Dev. 46 (6) (2002) 779–804.

[3] K.N. Rainey, S.M. You, Pool boiling heat transfer from plain and microporous, square pin-finned surfaces in saturated FC-72, J. Heat Transfer 122 (2000) 509–516.

[4] M. Arik, A. Bar-Cohen, Ebullient cooling of integrated circuits by Novec fluids, in: Proc. of the Pacific Rim Intersociety, Electronics Packaging Conf., Kauai, HI, 18–23 July 2001.

[5] W. Mathews, C. Lee, J. Peters, Experimental investigations of spray/wall impingement, Atomization Sprays 13 (2–3) (2003) 223–242.

[6] M. El-Genk, J. Parker, Pool boiling in saturated and subcooled HFE-7100 dielectric fluid from a porous graphite surface, in: Proc. 9th Intersociety Conf. on Thermal Phenomena, vol. 1, 2004, pp. 655–662.

[7] Y. Maydanik, S. Vershinin, M. Korukov, J. Octerbeck, Miniature loop heat pipes—a promising means for cooling electronics, in: Proc. 9th Intersociety Conf. on Thermal Phenomena, vol. 2, 2004, pp. 60–66.

[8] X. Chen, K. Toh, T. Wong, J. Chai, D. Pinjala, O. Navas, H. Ganesh, V. Kripesh, Direct liquid cooling of a stacked MCM, in: Proc. 9th Intersociety Conf. on Thermal Phenomena, vol. 1, 2004, pp. 199–206.

[9] J. Chang, S. You, A. Haji-Sheikh, Film boiling incipience at the departure from natural convection on flat, smooth surfaces, J. Heat Transfer 120 (1998) 402–409.
[10] M. El-Genk, H. Bostanci, Saturation boiling of HFE-7100 from a copper surface, Simulating a microelectronic chip, Int. J. Heat Mass Transfer 46 (2003) 1841–1854.
[11] M. El-Genk, H. Bostanci, Combined effects of subcooling and surface orientation on pool boiling of HFE-7100 from a simulated electronic chip, J. Exp. Heat Transfer 16 (2003) 281–301.
[12] G. Peterson, An Introduction to Heat Pipes: Modeling, Testing, and Applications, Wiley and Sons, New York, 1994.
[13] H. Ivey, Relationships between bubble frequency, departure diameter, and rise velocity in nuclear boiling, Int. J. Heat Mass Transfer 10 (1967) 1023–1040.
[14] B. Mikic, W. Rohsenow, A new correlation of pool-boiling data including the effect of heating surface characteristics, J. Heat Transfer 91 (1969) 245–250.
[15] C. Ramaswamy, Y. Joshi, W. Nakayama, W. Johnson, High-speed visualization of boiling from an enhanced structure, Int. J. Heat Mass Transfer 45 (2002) 4761–4771.
[16] J. Ramilison, P. Sadasivan, J. Lienhard, Surface factors influencing burnout on flat heaters, J. Heat Transfer 114 (1) (1992) 287–290.
[17] C. Baldwin, S. Bhavnani, R. Jaeger, Towards optimizing enhanced surfaces for passive immersion cooled heat sinks, in: Proc. Intersociety Conf. on Thermal and Thermotechnical Phenomena in Electronic Systems, 1998, pp. 399–407.
[18] H. Kubo, H. Takamatsu, H. Honda, Effects of size and number density of micro-reentrant cavities on boiling heat transfer from a silicon chip immersed in degassed and gas dissolved FC-72, J. Enhanced Heat Transfer 6 (2–4) (1999) 151–160.
[19] J. Tehver, Influences of porous coating on the boiling burnout heat flux, in: B. Sunden et al. (Eds.), Recent Advances in Heat Transfer, Elsevier Science Publishers, 1992, pp. 231–242.
[20] J. Chang, S. You, Heater orientation effects on pool boiling of microporous enhanced surfaces in saturated FC-72, J. Heat Transfer 118 (1996) 937–943.
[21] K. Rainey, S. You, S. Lee, Effect of pressure, subcooling, and dissolved gas on pool boiling from microporous surfaces in FC-72, J. Heat Transfer 125 (2003) 75–83.
[22] J. Chang, S. You, Enhanced boiling heat transfer from micro-porous surfaces: effects of a coating composition and method, Int. J. Heat Mass Transfer 40 (1997) 4449–4460.
[23] J. O'Connor, S. You, J. Chang, Gas-saturated pool boiling heat transfer from smooth and microporous surfaces in FC-72, J. Heat Transfer 18 (1996) 662–667.
[24] H. Honda, H. Takamastu, J. Wei, Enhanced boiling of FC-72 on silicon chips with micro-pin-fins and submicron scale roughness, J. Heat Transfer 124 (2002) 383–390.
[25] J. Wei, H. Honda, Effects of fin geometry on boiling heat transfer from silicon chips with micro-pin-fins immersed in FC-72, Int. J. Heat Mass Transfer 46 (2003) 4059–4070.
[26] Z. Liu, W. Lin, D. Lee, X. Peng, Pool boiling of FC-72 and HFE-7100, J. Heat Transfer 123 (2001) 399–400.
[27] A. Watwe, A. Bar-Cohen, A. McNeil, Combined pressure and subcooling effects on pool boiling from a PPGA chip package, J. Electron. Packag. 119 (1997) 95–105.
[28] F. Arbelaez, S. Sett, R. Mahajan, An experimental study on pool boiling of saturated FC-72 in highly porous aluminum foams, in: Proc. of 34th National Heat Transfer Conf., vol. 1, 2000, pp. 759–767.
[29] P. Marto, V. Lepere, Pool boiling heat transfer from enhanced surfaces to dielectric fluids, J. Heat Transfer 104 (1982) 292–303.
[30] S. You, T.W. Simon, A. Bar-Cohen, W. Tong, Experimental investigation of nucleate boiling incipience with a highly wetting dielectric fluid (R-113), Int. J. Heat Mass Transfer 33 (1990) 105–117.
[31] Y. Hong, C. Ammerman, S. You, Boiling characteristics of cylindrical heaters in saturated, gas saturated, and pure-subcooled FC-72, J. Heat Transfer 119 (1997) 313–318.
[32] M. El-Genk, J. Parker, Enhanced boiling of HFE-7100 dielectric liquid on porous graphite, Energy Conversion Manage. 46 (2005) 2455–2481.
[33] S. Kutateladze, Boiling heat transfer, Int. J. Heat Mass Transfer 4 (1961) 31–45.
[34] J. O'Connor, Enhancement of pool boiling heat transfer in highly wetting dielectric liquids, Ph.D. Dissertation, University of Texas at Arlington, Arlington, TX, 1994.
[35] A. McNiel, Pool boiling critical heat flux in a highly wetting liquid, Masters Thesis, University of Minnesota, Minneapolis, MN, 1992.
[36] H. Ivey, D. Morris, On the relevance of the vapor–liquid exchange mechanisms for subcooled boiling heat transfer at high pressure, Report AEEW-R137, United Kingdom Atomic Energy Authority, Winfrith, England, 1962.